J|A|C|S
ARTICLES
Published on Web 01/03/2002

Construction of Mixed Mercaptopropionic Acid/Alkanethiol Monolayers of Controlled Composition by Structural Control of a Gold Substrate with Underpotentially Deposited Lead Atoms

Katsuaki Shimazu,* Toshikazu Kawaguchi, and Takao Isomura

Contribution from the Division of Material Science, Graduate School of Environmental Earth Science, Hokkaido University, Sapporo 060-0810, Japan

Received November 27, 2000. Revised Manuscript Received August 15, 2001

Abstract: Mixed monolayers of 3-mercaptopropionic acid (MPA) and alkanethiols of various chain lengths have been constructed on Au based on a novel concept, namely, control of the composition of the component thiols in mixed monolayers by controlling the surface structure of the substrate. The Au substrate surface was first modified with underpotentially deposited Pb (UPD Pb) atoms, followed by the formation of a self-assembled monolayer (SAM) of alkanethiol. The UPD Pb atoms were then oxidatively stripped from the surface to create vacant site, on which MPA was adsorbed to finally form the mixed monolayers. The surface coverages of Pb, alkanethiol and MPA, and the total numbers of thiols were determined using an electrochemical quartz crystal microbalance, X-ray photoelectron spectroscopy, and reductive desorption voltammetry. These results demonstrate that the surface coverage of MPA in the mixed monolayers is determined by the initial coverage of UPD Pb. Fourier transform infrared spectra also support this conclusion. The observed single peak in the cyclic voltammogram for the reductive desorption shows that MPA and alkanethiol do not form their single-component domains. Scanning tunneling microscopy revealed the single-row pinstripe structure for all the thiol adlayers formed during each step of the preparation. This shows that the surface structure of the mixed monolayers is determined by the structure of the initially formed SAM on Au partially covered with UPD Pb.

Introduction

Mixed monolayers of alkanethiol derivatives are usually constructed by immersing the substrate into a mixed solution containing the corresponding precursor thiol molecules.[1−12] This is the simplest and easiest way to form mixed monolayers. However, it requires a number of trial-and-error experiments to obtain the desired composition because of the difference in adsorbability between component thiols. In the case where one of the thiols is preferentially adsorbed on the electrode, for example, the formation of a mixed monolayer with low surface concentration of that thiol is most difficult. Also, a difficulty exists in estimating the surface composition unless the thiol has an electroactive functionality. In addition, each component thiol is hardly mixed homogeneously and often forms a domain as shown by two waves in the cyclic voltammogram for the reductive desorption of the mixed monolayers.[13−15] Domain

* To whom correspondence should be addressed: (e-mail) shimazu@ees.hokudai.ac.jp; (phone) +81-11-706-2276; (fax) +81-11-706-4868.

(1) (a) Bain, C. D.; Whitesides, G. M. *J. Am. Chem. Soc.* **1988**, *110*, 3665. (b) Bain, C. D.; Whitesides, G. M. *J. Am. Chem. Soc.* **1988**, *110*, 6560. (c) Bain, C. D.; Whitesides, G. M. *J. Am. Chem. Soc.* **1989**, *111*, 7164. (d) Bain, C. D.; Evall. J.; Whitesides, G. M. *J. Am. Chem. Soc.* **1989**, *111*, 7155. (e) Bain, C. D.; Biebuyck, A. H.; Whitesides, G. M. *Langmuir* **1989**, *5*, 723. (f) Laibinis, P. E.; Whitesides, G. M. *Langmuir* **1990**, *6*, 87. (g) Laibinis, P. E.; Fox, M. A.; Folkers, J. P.; Whitesides, G. M. *Langmuir* **1991**, *7*, 3167. (h) Prime, K. L.; Whitesides, G. M. *Science* **1991**, *252*, 1164. (i) Pale-Grosdemange, C.; Simon, E. S.; Prime, K. L.; Whitesides, G. M. *J. Am. Chem. Soc.* **1991**, *113*, 12. (j) Laibinis, P. E.; Whitesides, G. M. *J. Am. Chem. Soc.* **1992**, *114*, 1990. (k) Folkers, J. P.; Laibinis, P. E.; Whitesides, G. M. *Langmuir* **1992**, *8*, 1330. (l) Laibinis, P. E.; Nuzzo, R. G.; Whitesides, G. M. *J. Phys. Chem.* **1992**, *96*, 5097. (m) Folkers, J. P.; Laibinis, P. E.; Whitesides, G. M. *J. Phys. Chem.* **1994**, *98*, 563.
(2) (a) Chidsey, C. E. D.; Bertozzi, C. R.; Putvinski, T. M.; Mujsce, A. M. *J. Am. Chem. Soc.* **1990**, *112*, 4301. (b) Chidsey, C. E. D. *Science* **1991**, *251*, 919.
(3) Haussling, L.; Michel, B.; Ringsdorf, H.; Rohrer, H. *Angew. Chem., Int. Ed. Engl.* **1991**, *30*, 569.
(4) (a) Evans, S. D.; Sharma, R.; Ulman, A. *Langmuir* **1991**, *7*, 156. (b) Ulman, A.; Evans, S. D.; Shnidman, Y.; Sharma, Y.; Eilers, J. E.; Chang, J. C. *J. Am. Chem. Soc.* **1991**, *113*, 1499.
(5) (a) Rowe, G. K.; Creager, S. E. *Langmuir* **1991**, *7*, 2307. (b) Creager, S. E.; Rowe, G. K. *Anal. Chim. Acta* **1991**, *246*, 233. (c) Creager, S. E.; Hockett, L. A.; Rowe, G. K. *Langmuir* **1992**, *8*, 854. (d) Rowe, G. K.; Creager, S. E. *Langmuir* **1993**, *9*, 2330. (e) Creager, S. E.; Rowe, G. K. *J. Electroanal. Chem.* **1994**, *370*, 203. (f) Rowe, G. K.; Creager, S. E. *J. Phys. Chem.* **1994**, *98*, 5500. (g) Creager, S. E.; Clarke, J. *Langmuir* **1994**, *10*, 3675. (h) Rowe, G. K.; Creager, S. E. *Langmuir* **1994**, *10*, 1186.
(6) Finklea, H. O.; Hanshew, D. D. *J. Am. Chem. Soc.* **1992**, *114*, 3173.
(7) Li, Y.; Huang, J.; Mclver, R. T., Jr.; Hemminger, J. C. *J. Am. Chem. Soc.* **1992**, *114*, 2428.
(8) (a) Evans, S. D.; Sanassy, P. *Thin Solid Films* **1994**, *243*, 325. (b) Sanassy, P.; Evans. S. D. *Langmuir* **1993**, *9*, 1024.
(9) Chailapakul, O.; Crooks, R. M. *Langmuir* **1993**, *9*, 884.
(10) (a) Bertilsson, L.; Liedberg, B. *Langmuir* **1993**, *9*, 141. (b) Atre, S. V.; Liedberg, B.; Allara, D. L. *Langmuir* **1995**, *11*, 3882.
(11) Stranick, S. J.; Parikh, A. N.; Tao, Y.-T.; Allara, D. L.; Weiss, P. S. *J. Phys. Chem.* **1994**, *98*, 7636.
(12) (a) Offord, D. A.; John, C. M.; Griffin, J. H. *Langmuir* **1994**, *10*, 761. (b) Offord, D. A.; John, C. M.; Linford, M. R.; Griffin, J. H. *Langmuir* **1994**, *10*, 883.
(13) Nishizawa, M.; Sunagawa, T.; Yoneyama, H. *J. Electroanal. Chem.* **1997**, *436*, 213.
(14) (a) Imabayashi, S.; Hobara, D.; Kakiuchi, T.; Knoll, W. *Langmuir* **1997**, *13*, 4502. (b) Hobara, D.; Sasaki, T.; Imabayashi, S.; Kakiuchi, T. *Langmuir* **1999**, *15*, 5073.
(15) Hobara, D.; Ota, M.; Imabayashi, S.; Niki, K.; Kakiuchi, T. *J. Electroanal. Chem.* **1998**, *444*, 113.

10.1021/ja004091b CCC: $22.00

formation, however, can be utilized in the architecture of different and more useful mixed monolayers. Such an approach has been reported by Kakiuchi et al.[14] They removed only one domain by setting the potential at the middle between the two waves to create adsorption sites for the new thiol. Thus, mixed monolayers of the new thiol and the thiol unremoved from the electrode surface can be formed. One of the advantages of this method will be that various mixed monolayers with the same domain size can be formed. According to their separate experiments,[15] only domains whose size exceeded 15 nm^2 produced two desorption waves. In other words, no homogeneously mixed monolayers at a molecular level or mixed monolayers with a domain size of <15 nm^2 can be formed by this method.

Domain size control is quite important for the analytical application of a well-ordered surface, because an analogue of a microarray electrode can be created by size control. However, control of the microenvironment around a single adsorbed molecule is required for application as an electrocatalyst and also for more fundamental studies such as the evaluation of the electron-transfer mechanism. For this purpose, the construction of homogeneously mixed monolayers or monolayers with very small domains becomes an important target. Use of an asymmetric disulfide is an elegant method for constructing such mixed monolayers.[16−18] It is principally guaranteed that the thiol fragment is homogeneously mixed, or if formed, the domain is very small at least just after the formation of the mixed monolayer. In fact, any experimental results which support domain formation were not obtained by scanning tunneling microscopy (STM),[17a] force microscopy,[18a] Fourier transform infrared (FT-IR) spectroscopy[17b] and reductive desorption voltammetry,[18b,c] unless mixed monolayers were prepared from very dilute solution[18b] or were annealed at elevated temperatures.[18a] However, the surface composition of mixed monolayers constructed by this method is principally limited to 1:1.

Our target is to create novel methodologies by which the mixed monolayers with controlled composition and distribution at a molecular level can be constructed. The structure of a self-assembled monolayer (SAM) is generally determined by the substrate−thiol bond, the lateral thiol-to-thiol interaction, and their relative intensity. The predominant factor that determines the distribution of thiols in a mixed monolayer prepared by a conventional immersion method is the lateral thiol-to-thiol interaction, because the same substrate−thiol bond is formed for both thiols. In the asymmetric disulfide method, the structure of the precursor molecule is a predominant factor, and the lateral thiol-to-thiol interaction may have some contribution to determine the local distribution around the thiol. In both cases, the structure or chemical properties of the adsorbate molecules determine the distribution of the thiols. The substrate does not play an important role in determining the distribution. However, we think that it is possible to use the substrate as a template for mixed monolayers by introducing heterogeneous sites on the substrate. In this paper, we describe a novel concept for the construction of mixed monolayers, namely, structural control of mixed SAMs by controlling the surface structure of the substrate at a molecular level. As a first approach to prove this concept, we have used underpotentially deposited (UPD) metals as heterogeneous sites on Au. Wrighton and co-workers constructed monolayers on interdigitated Au/ITO microarray electrodes by immersing the electrodes in the mixed solution of a thiol and a carboxylic acid (or a phosphonic acid).[19a] The immersion resulted in the selective attachment of the thiol to the Au electrode and a carboxylic acid (or a phosphonic acid) to the ITO electrode. This process was termed "orthogonal self-assembly". In their earlier work,[19b] Al_2O_3 was also used instead of ITO. Recently, Shabtai et al. reported the construction of mixed monolayers on $Au-SiO_2$ composites by successively dipping the composites in decanethiol and octadecane trichlorosilane solutions.[20] Their approaches are similar in concept to ours, because they attempted to control the component distribution via control of the surface composition. However, there are a couple of significant differences between their and our approaches. First, the sizes of the ITO microelectrode and the SiO_2 layer are 2 μm wide and 20−30 nm, respectively, so that the distribution of components cannot be controlled at a molecular level as we attempt to do. Second, the second-component electrode materials (ITO, SiO_2, Al_2O_3) remain after the construction of the mixed monolayers. This may not necessarily be a disadvantage for some applications of the mixed monolayers. In the case that the material is nonconducting (SiO_2, Al_2O_3), however, wider applications become possible if such a material is finally removed so that mixed monolayers are formed on a conducting and smooth substrate. In our method, the UPD metals are initially present, but mixed monolayers are constructed after the complete removal of the UPD metals or on a pure gold electrode.

It should be mentioned that several studies have been reported on the metal deposition into SAMs of alkanethiols and their derivatives. Most of the studies were conducted to estimate vacant sites in the SAMs[21] and to examine the influence of the SAM for UPD processes.[22−24] Oyamatsu et al. constructed mixed monolayers after the deposition of metal ions into alkanethiol SAMs.[25] Some of the UPD metals, such as Ag and Cu, form domains on the substrate Au electrode, and the alkanethiol adsorbed on the domain is desorbed at a potential different from that for the alkanethiol on Au. Therefore, it was possible to desorb either thiol to create adsorption sites for the new thiol. Thus, mixed monolayers could be formed. This is totally different from the present approach because the distribution of the UPD metal is governed by the structure of and interaction with the SAMs, which are hard to control at a

(16) Offord, D. A.; John, C. M.; Griffin, J. H. *Langmuir* **1994**, *10*, 761.
(17) (a) Takami, T.; Delamarche, E.; Michel, B.; Gerber, Ch.; Wolf, H.; Ringsdorf, H. *Langmuir* **1995**, *11*, 3876. (b) Schronherr, H.; Ringsdorf, H. *Langmuir* **1996**, *12*, 3891. (c) Schronherr, H.; Ringsdorf, H.; Jaschke, M.; Butt, H.-J.; Bamberg, E.; Allinson, H.; Evans, S. D. *Langmuir* **1996**, *12*, 3898.
(18) (a) Ishida, T.; Yamamoto, S.; Mizutani, W.; Motomatsu, M. Tokumoto, H.; Hokari, H.; Azehara, H.; Fujihira, M. *Langmuir* **1997**, *13*, 3261. (b) Azehara, H.; Yoshimato, S.; Hokari, H.; Akiba, U.; Taniguchi, I.; Fujihira, M. *Electrochemistry* **1999**, *67*, 1227. (c) Azehara, H.; Yoshimato, S.; Hokari, H.; Akiba, U.; Taniguchi, I.; Fujihira, M. *J. Electroanal. Chem.* **1999**, *473*, 68.
(19) (a) Gardner, T. J.; Frisbie, C. D.; Wrighton, M. S. *J. Am. Chem. Soc.* **1995**, *117*, 6927. (b) Labinis, P. E.; Hickman, J. J.; Wrighton, M. S.; Whitesides, G. M. *Science*, **1989**, *245*, 845.
(20) Shabtai, K.; Cohen, S.; Cohen, H.; Rubinstein, I. 197th Electrochemical Society Meeting, Toronto, Canada, 2000; Abstract 1122.
(21) Sun, L.; Crooks, R. M. *J. Electrochem. Soc.* **1991**, *138*, L23.
(22) (a) Gilbert, S. E.; Cavalleri, O.; Kern, K. *J. Phys. Chem.* **1996**, *100*, 12123. (b) Cavalleri, O.; Gilbert, S. E.; Kern, K. *Surf. Sci.* **1997**, *377*, 931.
(23) (a) Whelan, C. M.; Smyth, M. R.; Barnes, C. J. *J. Electroanal. Chem.* **1998**, *441*, 109. (b) Whelan, C. M.; Smyth, M. R.; Barnes, C. J. *Langmuir* **1999,** *15*, 116.
(24) Hagenstrom, H.; Schneeweiss, M. A.; Kolb, D. M. *Langmuir* **1999**, *15*, 7802.
(25) Oyamatsu, D.; Nishizawa, M.; Kuwabata, S.; Yoneyama, H. *Langmuir* **1998**, *14*, 3298.

molecular level. On the other hand, the structure of the UPD metal on bare metal electrodes is well characterized and the amount of it is easy to control by the electrode potential.[26] In addition, it is known that the UPD metal is commonly in a well-ordered structure on single-crystal electrodes. Therefore, the preassembly UPD is essentially different from postassembly UPD in the ability to control the distribution and amount of heterogeneous sites. The single-component and mixed-thiol monolayers have also been constructed on Ag and Cu underpotentially deposited on gold.[27−29] However, the UPD metal was not used as a template, because the monolayers were simply prepared by a conventional immersion method. In these studies, only the stability of the monolayers was examined.

Experimental Section

Materials. Reagent grade 3-mercaptopropionic acid (MPA) was purchased from Kanto Chemicals. Octanethiol, dodecanethiol, and octadecanethiol of reagent grade were obtained from TCI (Tokyo Chemical Industry). Chemicals such as KOH (Wako), $NaClO_4$ (Wako), PbO (Kanto), $(CH_3COO)_2Pb$ (Wako), and $PbCl_2$ (Kanto) were of reagent grade. Sulfuric acid (Wako Pure Chemicals) was of Suprapure grade. All aqueous solutions were prepared with Milli-Q water and were deaerated sufficiently with argon of 5 N purity prior to use. Absolute ethanol (Wako Pure Chemicals) of reagent grade was used as a solvent for the SAM preparation. All chemicals were used as received.

Substrate Preparation. The substrate for the mixed monolayers was a 200-nm gold thin film, which was evaporated in a vacuum onto a slide glass maintained at 160 °C. To improve the adhesion of the gold film to the slide glass, 10 nm of a Ti film was evaporated prior to the Au deposition. For electrochemical quartz crystal microbalance (EQCM) measurements, a 200-nm gold thin film was prepared on a 5-MHz, AT-cut quartz crystal wafer (Maxtek Co.) according to the procedure reported previously.[30] The gold films, flame-annealed immediately before use,[31] showed the typical characteristics of Au(111) for the electrochemical formation/reduction of the surface oxide in 1 M H_2SO_4 as reported previously.[30] Predominant growth of Au(111) on these substrates has also been reported in the literature.[32−34] The roughness factor of the gold, determined from the charge required for the reduction of the surface oxide,[35] ranges from 1.1 to 1.5, dependent on conditions of vacuum evaporation such as base pressure (7×10^{-7}−2×10^{-5} mmHg), substrate temperature for Ti deposition (160−300 °C), substrate (quartz or slide glass), and evaporation rate of Au (0.2−0.05 Å s^{-1}). A couple samples were selected from those prepared simultaneously and were used for the determination of the roughness factor.

Electrochemistry and EQCM. Cyclic voltammetry and potential step experiments were performed in a three-electrode cell using an EG&G Princeton Applied Research model 273A potentiostat. The reference electrode was a Ag/AgCl (saturated KCl) electrode, and all potentials in the text are referred to this electrode. A platinized platinum foil served as a counter electrode. Current and potential were recorded by a personal computer. All measurements were carried out in an Ar-filled glovebox.

Scheme 1. Construction of Mixed Monolayers of Controlled Compositions

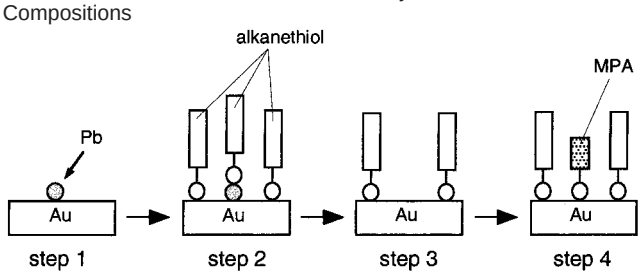

The EQCM measurements were conducted using a Maxtek model TPS-550 QCM sensor head, in which the Au/quartz crystal was mounted, and a Hewlett-Packard model 53131A frequency counter. Frequency data were analyzed based on Sauerbrey's equation.[36−38] For a 5-MHz quartz crystal used in this study, the frequency change of 1 Hz corresponds to 17.7×10^{-9} g cm^{-2}. The impedance measurements of the quartz crystal were conducted using a Hewlett-Packard model E5100A Network Analyzer to examine the possible contribution of viscoelastic changes at the interface to the frequency change.[37−40] No detectable change in the equivalent circuit resistance is observed, showing that the observed frequency change is directly proportional to the change in mass and is not a convolution of mass and viscoelastic changes.

X-ray Photoelectron Spectroscopy (XPS). The X-ray photoelectron spectra (XP spectra) were obtained using a Rigakudenki model XPS-7000 X-ray photoelectron spectrometer with monochromic Mg Kα radiation at 25−300 W. The takeoff angle was 90°. The Au $4f_{7/2}$ emission was used as the internal reference to determine the binding energies of the elements.

Fourier Transform Infrared Spectroscopy. FT-IR spectra were obtained in the external reflection mode using p-polarized light incident at 82° with a resolution of 4 cm^{-1} using a Biorad FTS 60A/816 spectrometer equipped with a liquid nitrogen-cooled MCT detector. Typically, 1024 scans were averaged. Freshly prepared gold films were used to obtain the reference spectra.

Scanning Tunneling Microscopy. A Au(111) facet of the single-crystal Au bead prepared by flaming the end of a Au wire was used as a STM scanning plane. All STM images were acquired with a Digital Instruments Nanoscope III STM (Santa Barbara, CA). The instrument was equipped with a low-current converter (Digital Instruments model MMSTMLC) and was operated in the laboratory ambient atmosphere. For imaging, mechanically cut Pt−Ir wires were used. All images were obtained at constant tunneling current (10−100 pA) with bias voltages of 0.7−1.0 V.

Results and Discussion

The procedures for the construction of mixed monolayers with controlled compositions are schematically presented in Scheme 1. They consist of four steps: (step 1) UPD of lead ions onto the Au electrode, (step 2) the formation of an alkanethiol SAM on Au and probably also on the UPD Pb atoms, (step 3) desorption of the UPD Pb atoms, and (step 4) adsorption of MPA to form the mixed monolayer. There are a couple reasons for choosing Pb as the UPD metal. First, the UPD Pb is oxidatively desorbed at lower electrode potentials than the

(26) Kolb, D. M.; Gerisher, H.; Tobias, C. In *Advances in Electrochemistry and Electrochemical Engineering*; Gerischerand, H., Tobias, C. W., Eds.; J. Wiley and Sons: New York, 1978; Vol. 11.
(27) Burgess, J. D.; Hawkridge, F. M. *Langmuir* **1997**, *13*, 3781.
(28) (a) Jennings, G. K.; Laibinis, P. E. *J. Am. Chem. Soc.* **1997**, *119*, 5208. (b) Jennings, G. K.; Laibinis, P. E. *Langmuir* **1996**, *12*, 6173.
(29) Zamborini, P. Z.; Campbell, J. K.; Crooks, R. M. *Langmuir* **1998**, *14*, 640.
(30) Kawaguchi, T.; Yasuda, H.; Shimazu, K.; Porter, M. D. *Langmuir* **2000**, *16*, 9830.
(31) In the case of the Au/quartz crystal, it was essential to prevent direct contact of the Au/quartz with the flame to maintain the piezoelectric properties unchanged.
(32) Borges, G. L.; Kanazawa, K. K.; Gordon, J. G.; Ashley, K.; Richer, J. *J. Electroanal. Chem.* **1994**, *364*, 281.
(33) Watanabe, M.; Uchida, H.; Miura, M.; Ikeda, N. *J. Electroanal. Chem.* **1995**, *384*, 191.
(34) Uosaki, K.; Ye, S.; Naohara, H.; Oda, Y.; Haba, T.; Kondo, T. *J. Phys. Chem.* **1997**, *101*, 7566.
(35) Angerstein-Kozlowska, H. A.; Conway, B. E.; Hamelin, A.; Stoicoviu, L. *J. Electroanal. Chem.* **1987**, *228*, 429.
(36) Sauerbrey, G. Z. *Z. Phys.* **1959**, *155*, 206.
(37) Buttry, D. A.; Ward, M. D. *Chem. Rev.* **1992**, *92*, 1355.
(38) Thompson, M.; Kipling, A. L.; Duncan-Hewitt, W. C.; Rajakovic, L. V.; Cavic-Vlasak, B. A. *Analyst* **1991**, *116*, 881.
(39) Muramatsu, H.; Karube, I. *Anal. Chem.* **1988**, *60*, 2142.
(40) Oyama, N.; Ohsaka, T. *Prog. Polym. Sci.* **1995**, *20*, 761.

alkanethiols so the removal of the UPD Pb can be performed without the desorption of the alkanethiol. Second, the structure of the UPD Pb on Au(111) was well examined by several groups.[41−51] At a full monolayer, the lead is ordered in hexagonal closed pack geometry[41,44,46bc,48,49,51] rotated by 2−5° with respect to the Au lattice.[49,51] In early studies, it was reported that the lead arrays in a $p(\sqrt{3}\times\sqrt{3})R30°$ structure at relatively low surface concentration.[41b,44,45] This structure is the same as that of the alkanethiols in SAMs.[52−56] Therefore, the partial replacement of the UPD Pb with alkanethiol is possible without rearrangement of the remaining UPD Pb. This means that the UPD Pb serves as an ideal template. However, recent STM and atomic force microscopy (AFM) studies reveal that the lead forms islands at the initial stage of the deposition.[47,49,51] The typical size of the islands is 1.5−5 nm. If islands of this size are formed, the monolayers mixed homogeneously at a molecular level will be never obtained. However, the size is still much smaller than the domain size in mixed monolayers prepared by conventional methods. Interestingly, we have never observed domains of this size and larger in STM images of mixed monolayers prepared by our method as described later.

Underpotential Deposition of Lead Ion (Step 1). The underpotential deposition of lead ion (Pb^{2+}) was performed in 0.2 M $NaClO_4$ containing 1 mM Pb^{2+}. Figure 1a shows the cyclic voltammogram on a gold QCM electrode in 0.2 M $NaClO_4$ + 1 mM $PbCl_2$. Although redox waves are broader, the voltammogram is similar in shape to those taken on Au electrodes in aqueous solutions.[43,46a,47d] Particularly, a peak splitting of both cathodic and anodic waves at about −0.2 to −0.15 V is observed for the UPD of Pb^{2+} on Au(111) in acidic solutions. The deposition starts at around 0.1 V versus Ag/AgCl as shown by the increase in cathodic current and is completed at −0.4 V. The frequency response agrees well with current response (Figure 1b); onset potentials are the same between current and frequency, and a large frequency decrease is observed at the main waves. The mpe, defined as the mass change per mole of electrons, was calculated using the following equation,

$$\text{mpe} = \Delta f S/(Q_{\text{Pb}}/F) \qquad (1)$$

where Δf and Q_{Pb} represent the total frequency change (Hz) and the total deposition charge (C cm^{-2}) during the UPD, respectively, and F is the Faraday constant. The proportionality constant, S, is 17.7×10^{-9} g cm^{-2} Hz^{-1} for 5-MHz, AT-cut quartz crystals. The mpe is equal to the molar mass of the deposited species if desorption is a one-electron process. The mpe determined from the results shown in Figure 1 is 105 g mol^{-1}. Assuming a two-electron deposition, the mass of the deposited species becomes 210 g mol^{-1}, which is very close to the atomic weight of Pb (207.2). The mpe value is independent of the lead compound used: 108 and 100 g mol^{-1} for $(CH_3COO)_2Pb$ and PbO, respectively. These results show a simple deposition of lead ion without the co-deposition of electolyte ions. Similar EQCM results have been reported for UPD of Pb^{2+} in a perchloric acid solution.[46a]

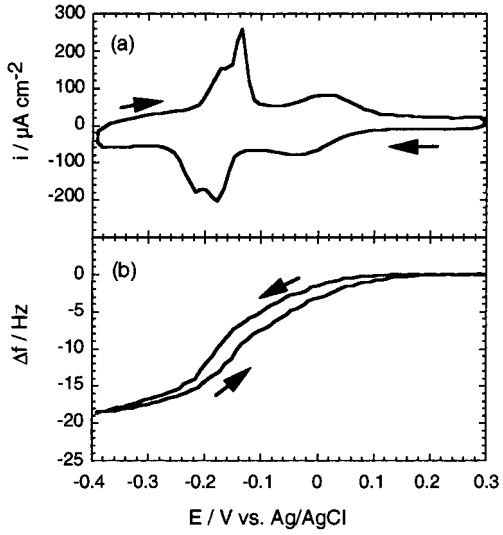

Figure 1. EQCM response for underpotential deposition of Pb^{2+} in 1 mM $PbCl_2$ + 0.2 M $NaClO_4$. Sweep rate, 0.10 V s^{-1}. (a) Current and (b) frequency change.

To control the amount of UPD Pb, the deposition was performed at various potentials using a double potential step or a single potential step method. In the double potential step experiments, the electrode potential was first stepped from 0.3 to −0.4 V and then to the preset deposition potential. In the single-step method, the first step of the double potential step method was omitted. Both methods gave the same results. After the lead ion was deposited at a given potential, the UPD Pb was stripped by a linear sweep voltammetry to estimate the amount of UPD Pb. Stripping voltammograms and frequency responses from various deposition potentials are shown in Figure 2a and b, respectively. As expected, both the peak intensity and frequency change increased with the decrease in the deposition potential. The total stripping charge and total frequency change are plotted as a function of deposition potential in Figure 2c. Both agree well with each other, showing that the mpe is independent of the electrode potential. The maximum and saturated values are obtained at −0.40 V. The charge at this potential (270 μC cm^{-2}) is within the values (225−320 μC cm^{-2}) reported for the Pb monolayer in the literature.[43−45,46a,47a,d,57,58] The surface coverage of the UPD Pb at

(41) (a) Beberian, J. P.; Rheed, G. E. *J. Phys. F* **1973**, *3*, 675. (b) Perdereau, J.; Beberian, J. P.; Rheed, G. E. *J. Phys. F* **1974**, *4*, 798. (c) Beberian, J. P. *Surf. Sci.* **1978**, *74*, 437.
(42) Snyman, H. C.; Boswell, F. W. *Surf. Sci.* **1974**, *41*, 21.
(43) Adzic, R.; Yeager, E.; Cahan, B. D. *J. Electrochem. Soc.* **1974**, *121*, 474.
(44) Schultze, J. W.; Dickertmann, D. *Surf. Sci.* **1976**, *54*, 489.
(45) (a) Ganon, J. P.; Clavilier, J. *Surf. Sci.* **1984**, *145*, 487. (b) Ganon, J. P.; Clavilier, J. *Surf. Sci.* **1984**, *147*, 583.
(46) (a) Melroy, O. R.; Kanazawa, K.; Gordon, J. G., II; Buttry, D. *Langmuir* **1986**, *2*, 697. (b) Samant, M. G.; Toney, M. F.; Borges, G. L.; Blum, L.; Melroy, O. R. *J. Phys. Chem.* **1988**, *92*, 220. (c) Toney, M. F.; Gordon, J. G.; Samant, M. G.; Borges, G. L.; Melroy, O. R.; Yee, D.; Sorensen, L. B. *J. Phys. Chem.* **1995**, *99*, 473.
(47) (a) Green, M. P.; Richter, M.; Xing, X.; Scherson, D.; Hanson, K. J.; Ross, P. N., Jr.; Carr, R.; Lindau, I. *J. Microscopy* **1988**, *152*, 823. (b) Green, M. P.; Hanson, K. J.; Scherson, D.; Xing, X.; Richter, M.; Ross, P. N.; Carr, R.; Lindau, I. *J. Phys. Chem.* **1989**, *93*, 2181. (c) Green, M. P.; Hanson, K. J.; Carr, R.; Lindau, I. *J. Electrochem. Soc.* **1990**, *137*, 3493. (d) Green, M. P.; Hanson, K. J. *Surf. Sci.* **1991**, *259*, L743.
(48) Fleischmann, M.; Mao, B. W. *J. Electroanal. Chem.* **1988**, *247*, 297.
(49) Tao, N. J.; Pan, J.; Li, Y.; Oden, P. I.; DeRose, J. A.; Lindsay, S. M. *Surf. Sci.* **1992**, *271*, L338.
(50) Chabala, E. D.; Harji, B. H.; Rayment, T.; Archer, M. D. *Langmuir* **1992**, *8*, 2028.
(51) Chen, C.; Washburn, N.; Gewirth, A. A. *J. Phys. Chem.* **1993**, *97*, 9754.
(52) Chidsey, C. E. D.; Liu, G.-Y.; Rowntree, P.; Scoles, G. *J. Chem. Phys.* **1981**, *91*, 4421.
(53) Widrig, C. A.; Alves, C. A.; Porter, M. D. *J. Am. Chem. Soc.* **1991**, *113*, 2807.
(54) Samant, M. G.; Brown, C. A.; Gordon, J. G. *Langmuir* **1991**, *7*, 437.
(55) Kim, Y.-T.; McCarley, R. L.; Bard, A. J. *J. Phys. Chem.* **1992**, *96*, 7416.
(56) Dubois, L. H.; Zegarski, B. R.; Nuzzo, R. G. *J. Chem. Phys.* **1993**, *98*, 678.

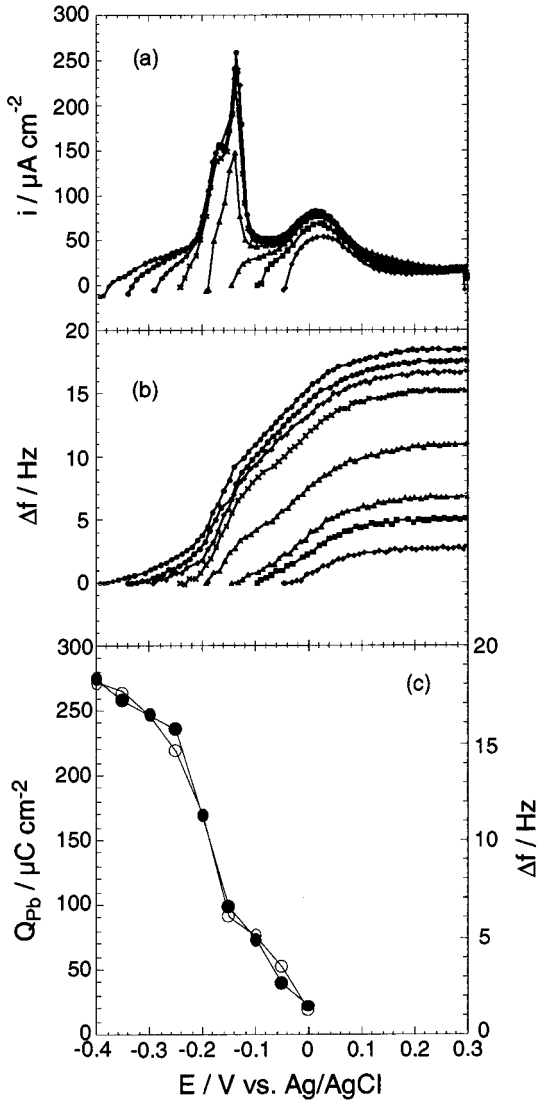

Figure 2. (a) Stripping voltammograms of UPD Pb, (b) simultaneously obtained frequency changes in 0.2 M NaClO4, and (c) UPD potential dependences of oxidation charge (open circle) and frequency change (solid circle). The lead ion was deposited at −0.40, −0.35, −0.30, −0.25, −0.20, −0.15, −0.10, and −0.05 V in 1 mM $PbCl_2$ + 0.2 M $NaClO_4$. Sweep rate, 0.10 V s^{-1}.

each deposition potential was given by the ratio of the amount of Pb at that potential to the saturated value. In the following experiments, two samples different in surface coverage were prepared by setting the deposition potentials at −0.2 and −0.1 V versus Ag/AgCl. The average surface coverages at these deposition potentials are 0.60 and 0.30, respectively. These values are referred to hereafter as the initial Pb coverage, θ_{Pb}^0.

Self-Assembly of Alkanethiol (Step 2). After the UPD of Pb^{2+} at a given potential for 1 min, the Pb^{2+} solution was replaced with a fresh and deaerated 0.2 M $NaClO_4$ solution several times. During the replacement, the electrode was kept at the deposition potential to avoid any unexpected oxidative desorption of the UPD Pb. An ethanolic solution of alkanethiol (2 mM) was then injected into the $NaClO_4$ solution to form the SAM on Au and also probably on the UPD Pb on Au. The final concentration was 0.2 mM.[59] In some other experiments,

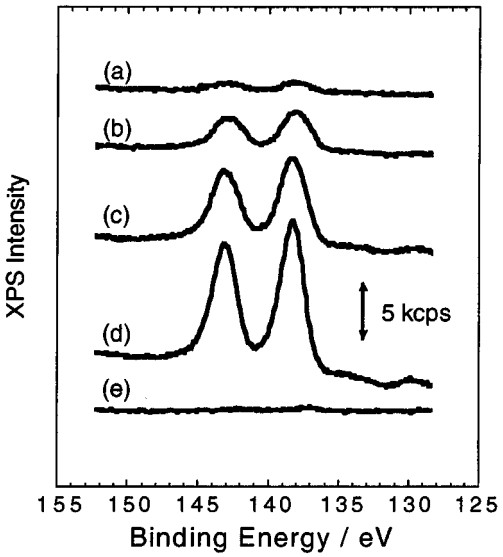

Figure 3. XPS Pb 4f spectra of octadecanethiol SAM-covered electrodes (a−d) before and (e) after desorption of UPD Pb. Deposition potentials of UPD Pb: (a) 0.20, (b) −0.10, (c, e) −0.20, and (d) −0.40 V. The desorption of UPD Pb was conducted at 0.50 V.

the ethanolic solution of alkanethiol was injected just after the UPD of Pb^{2+} without solution replacement with fresh 0.2 M $NaClO_4$.[60] Both procedures gave the same results. After 1-min contact with the dilute thiol solution, the electrode was removed from the solution and then washed several times with 2 mM thiol solution. The electrode was further immersed in 2 mM thiol solution for 1 h to complete the formation of the monolayer. The SAM-coated electrodes were sufficiently rinsed with ethanol and water.

Typical XPS Pb 4f spectra of octadecanethiol-coated electrodes are shown in Figure 3. The Pb 4f signal increases in intensity with the decrease in the deposition potential. The Pb 4f signal was integrated and then normalized to the integrated Au 4f signal. From the signal intensity thus obtained, we calculated the surface coverage of Pb, which is defined as the ratio of the Pb 4f intensity to that for the Pb monolayer. The average surface coverages of Pb are 0.64 and 0.27 at UPD potentials of −0.2 and −0.1 V, respectively. These values are essentially the same as those obtained by stripping voltammetry before the SAM formation or the initial Pb coverages. Therefore, it is concluded that almost all of the UPD Pb atoms remained on the electrode surface during the self-assembly process.

Tracings a and b of Figure 4 show the FT-IR spectra of the octadecanethiol SAMs on a bare gold electrode and Pb-coated gold electrode ($\theta_{Pb}^0 = 0.60$), respectively. The spectrum of an octadecanethiol SAM on Au is the same as those in the literature.[61,62] The bands at 2918 and 2851 cm^{-1} are attributed to $\nu_a(CH_2)$ and $\nu_s(CH_2)$, respectively. The other bands at 2963, 2937 (shoulder), and 2878 cm^{-1} are assigned to $\nu_a(CH_3$, ip) and $\nu_s(CH_3)$ (the latter two bands are split due to the Fermi resonance). The octadecanethiol SAM formed on the Pb-coated gold electrode gives essentially the same spectrum in peak position and intensity as the octadecanethiol SAM on Au. This

(57) Hamelin, A. *J. Electroanal. Chem.* **1979**, *101*, 285.
(58) Vicente, V. A.; Bruckenstein, S. *Anal. Chem.* **1973**, *45*, 2036.
(59) The $NaClO_4$ solution became hazy when the octadecanethiol solution was added.
(60) In the presence of Pb^{2+} in the solution, a precipitate was slightly formed.
(61) Porter, M. D.; Bright, T. B.; Allara, D. L.; Chidsey, C. E. D. *J. Am. Chem. Soc.* **1987**, *109*, 3559.
(62) Ulman, A. *J. Mater. Ed.* **1989**, *11*, 205.

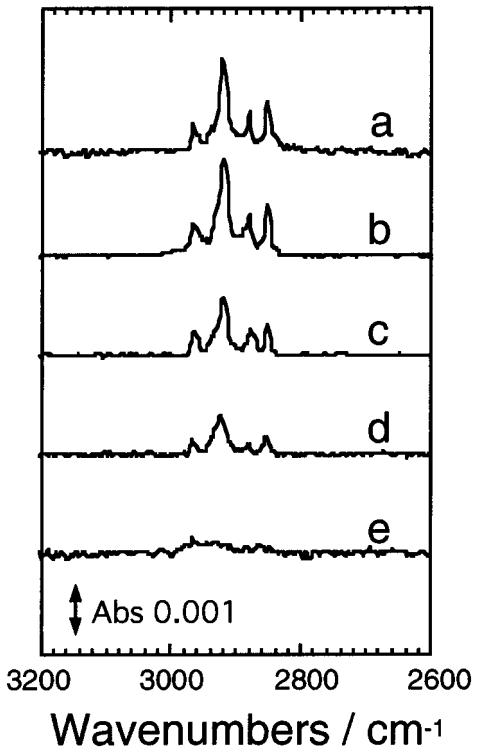

Figure 4. FT-IR spectra of (a) octadecanethiol SAM on Au, (b) octadecanethiol SAM on UPD Pb/Au, (c) octadecanethiol adlayer remaining after the desorption of UPD Pb, (d) mixed octadecanethiol/MPA monolayer, and (e) MPA SAM on Au. The initial Pb coverage for (b−d) is 0.60.

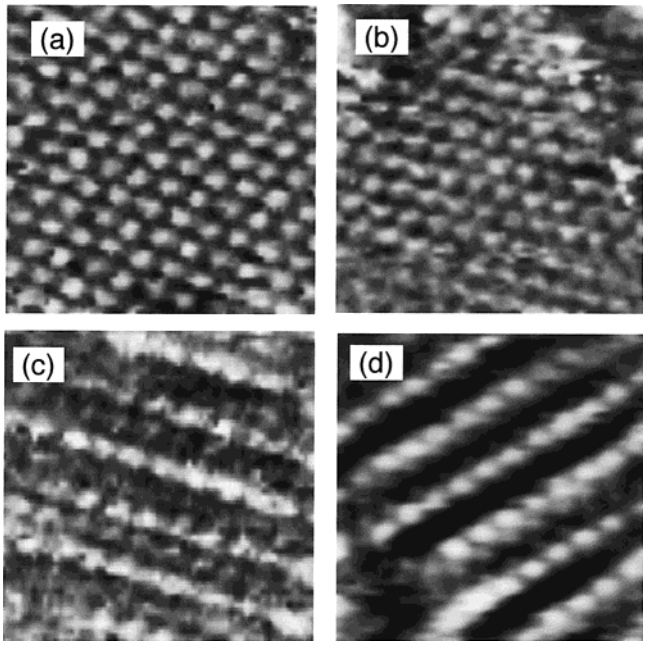

Figure 5. The 5 nm × 5 nm STM images of the (a) octanethiol SAM on Au, (b) octanethiol SAM on UPD Pb/Au ($\theta_{Pb}^0 = 1.00$), (c) octanethiol SAM on UPD Pb/Au ($\theta_{Pb}^0 = 0.60$), and (d) octanethiol adlayer remained after the desorption of UPD Pb ($\theta_{Pb}^0 = 0.60$).

indicates that octadecanethiol is adsorbed both on Au and UPD Pb.

The high-resolution STM image of the octanethiol SAMs formed on Au fully covered with UPD Pb ($\theta_{Pb}^0 = 1.00$) shows spots with hexagonal symmetry and the nearest-neighbor spacing of 0.49 nm (Figure 5b), which is consistent with the $(\sqrt{3}\times\sqrt{3})R30°$ structure. As reported in the literature,[53,55] an octanethiol SAM on Au also has the $(\sqrt{3}\times\sqrt{3})R30°$ structure (Figure 5a). Thus, SAMs of the same structure are formed whether or not the UPD Pb exists on the surface. Figure 5c shows the STM image of an octanethiol SAM on Au partially covered with UPD Pb ($\theta_{Pb}^0 = 0.60$). The pinstripe structure is observed in which the rows of brighter and dimmer spots alternately appear. The periodicity of spots along each row is 0.50 nm, which is almost the same as the intermolecular spacing of the $(\sqrt{3}\times\sqrt{3})R30°$ structure. The spacing between two adjacent rows of brighter (or dimmer) spots is ∼0.87 nm, which is consistent with the next-nearest-neighbor spacing in the $(\sqrt{3}\times\sqrt{3})R30°$ structure. Such a pinstripe structure is described as the $(1\times\sqrt{3})$ structure according to the notation established by Poirier et al.[63] Because there exist two kinds of adsorbed octadecanethiols (one on Au and the other on UPD Pb), it is reasonable to assume that one of the adsorbed thiols gives brighter spots and the other gives dimmer spots. This implicitly means that UPD Pb atoms are also aligned in rows to form the pinstripe structure. Therefore, the pinstripe structure observed for the SAM on UPD Pb/Au ($\theta_{Pb}^0 = 0.60$) is regarded as one in which the octanethiol and the octanethiol-adsorbed UPD Pb alternately occupy rows in the $(\sqrt{3}\times\sqrt{3})R30°$ structure. Although the $(\sqrt{3}\times\sqrt{3})R30°$ structure was reported for UPD Pb on Au based on electrochemical data,[41b,44,45] islands of typically 1.5−5 nm[47,49] and rarely 16 nm[51] were recently observed in the STM images. Once large islands are formed, it is not plausible that the deposited Pb rearranges to form the pinstripe. Therefore, we think that the lead should be atomically and uniformly dispersed or in very small islands at the beginning (step 1), inconsistent with these STM results. Because it is reported that the structure of UPD Pb on Au is dependent on the deposition conditions,[49] it is important to obtain in situ STM images of the UPD Pb on Au under the present conditions. These experiments are currently underway.

Desorption of UPD Pb Atoms (Step 3). The oxidative desorption of UPD Pb was performed in an aqueous $NaClO_4$ solution by setting the electrode potential of SAM-coated Pb/Au at 0.5 V. After keeping the potential for 30 min, the electrode was removed from the solution, followed by sufficient rinsing with water. Figure 3e shows the XPS Pb 4f spectrum after desorption of the UPD Pb, the initial coverage of which is 0.60. It is clear from the figure that the Pb atoms are completely removed.

After desorption of the UPD Pb, the reductive desorption of the SAM was performed in 0.5 M KOH solution to estimate the amount of the thiol remaining on the electrode surface. The reductive desorption is known to be a one-electron process, and therefore, the amount of adsorbed thiol can be determined straightforwardly from the desorption charge.[64−68] To estimate the desorption charge accurately, we have paid special attention to estimate the charge due to the double-layer charging, because the contribution of the latter usually reaches ∼30% of the total charge and cannot be negligible.[30,66,68] The double-layer charge was estimated using the following equation,[30]

$$Q_{dl} = [(-1.25 - PZC_{Au})C_{Au}] - [(-0.40 - PZC_{adlayer})C_{adlayer}] \quad (2)$$

where C and PZC are the capacitance and the potential of zero charge, respectively, of the Au or adlayer shown in the subscript.

Table 1. PZCs and Capacitances of Alkanethiol Adlayers after Desorption of UPD Pb and Mixed Monolayers

	C8 adlayers[a]		C8/MPA[b]		C12/MPA[b]		C18/MPA[b]	
θ_{Pb}^0	PZC	*C*	PZC	*C*	PZC	*C*	PZC	*C*
0	0.26	7.5	0.25	15	0.27	11	0.30	3.2
0.30	0.09	34	0.13	21	0.13	14	0.16	15
0.60	−0.08	35	0.02	30	0.02	22	0.04	19
1.0	−0.31	40	−0.14	41	−0.14	41	−0.14	41

[a] After desorption of UPD Pb. [b] Mixed monolayers. PZCs and capacitances (*C*) are shown in V vs Ag/AgCl and μF cm^{-2}, respectively. C8, C12, and C18 represent octanethiol, dodecanethiol, and octadecanethiol, respectively.

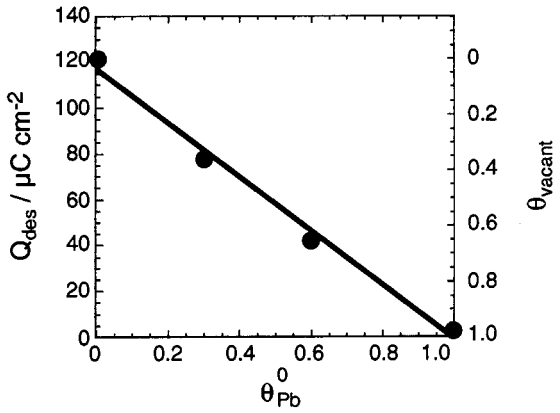

Figure 6. Desorption charge of octanethiol after the removal of UPD Pb as a function of the initial Pb coverage.

Numerical values of −0.4 and −1.25 appeared in the equation, because the current was integrated in the potential range from −0.4 to −1.25 V. We measured the PZCs and capacitances of partially covered adlayers using cyclic voltammetry in a KOH solution according to the procedure in the literature.[69] Results are summarized in Table 1. The desorption charge, Q_{des} was then calculated by subtracting Q_{dl} and also the charge due to hydrogen evolution from the total charge (detailed procedures have been reported previously[30]). Q_{des} thus determined was plotted versus the initial Pb coverage in Figure 6. When the deposition potential was set at 0.1 V, no Pb was deposited ($\theta_{Pb}^0 = 0$) as shown in Figure 1. As a result, the alkanethiol SAM with a full coverage is expected to form just as an ordinal SAM. Taking into account the roughness factor (1.35) of the Au film electrodes used in these experiments, the desorption charge is calculated to be 89 μC cm^{-2}(real area). This is close to the value expected for the $(\sqrt{3}\times\sqrt{3})R30°$ structure. In the case where Pb was deposited at −0.4 V, a full monolayer of Pb is formed and no adsorption site for alkanethiol remains on Au. After the Pb desorption, therefore, it is expected that nothing is left and that the surface becomes that of bare gold. In fact, the Q_{des} value is very small (2.3 μC cm^{-2}). The nonzero Q_{des} value is probably due to the readsorption of the desorbed thiol that was not washed off during rinsing. For the other adlayers, Q_{des}, and also pzc and capacitances, are between those of bare Au and the alkanethiol SAM with full coverage, showing the partial coverages by the alkanethiol. As shown in Figure 6, Q_{des} decreases linearly with the initial Pb coverage. Conversely, the surface fraction of vacant sites ($\theta_{vacant} = 1 - Q_{des}/Q_{des,full\ coverage}$), which is covered with neither alkanethiol nor Pb, increases linearly with the initial Pb coverage. The fractions of vacant sites are 0.52 and 0.27 for the samples of $\theta_{Pb}^0 = 0.60$ and 0.30, respectively. This indicates that the same fraction of vacant sites as that of the Pb deposited at the initial step is created by the desorption of the octanethiol-adsorbed UPD Pb.

The partial desorption of thiols is also confirmed by FT-IR spectroscopy and STM. Figure 4c shows an FT-IR spectrum of an octadecanethiol adlayer formed by the desorption of UPD Pb ($\theta_{Pb}^0 = 0.60$). The intensity of all IR bands observed in a C−H stretching region became smaller compared with that before the desorption of UPD Pb, showing the desorption of octadecanethiol adsorbed on UPD Pb. However, the decrease in the intensity (average 45% for three independent samples) is not as large as that (60%) expected from the quantitative desorption of octadecanethiol adsorbed on UPD Pb. Because the quantitative desorption was evidenced by XPS and reductive desorption, the stronger peak intensity is probably due to the change in the orientation of the alkyl chain from a more perpendicular to a more parallel one. This may be induced by losing the neighboring rows.

Figure 5d shows the STM image of the electrode surface at this stage. Although the pinstripe structure is observed, the dimmer spots, which were observed before the desorption of UPD Pb, disappeared. The periodicity of spots along the row and the spacing between two adjacent rows remained unchanged. These results are consistent with the desorption of octanethiol adsorbed on the UPD Pb and the resulting formation of vacant sites. Thus the remaining spots are attributed to the octanethiol adsorbed on Au.

In the following step, we use these vacant sites as the adsorption sites for MPA to construct the mixed monolayers.

Formation of a Mixed Monolayer (Step 4). The Au electrode partially covered with alkanethiol was immersed in a 1 mM ethanolic solution of MPA for 1 h. The mixed monolayers thus formed were characterized by reductive desorption, XPS, FT-IR, and STM.

Figure 7 shows linear sweep voltammograms for reductive desorpton of mixed monolayers of MPA and alkanethiols in 0.5 M KOH, together with the corresponding single-component monolayers. In addition to the main desorption wave, a small shoulder or wave (subwave) was observed at more negative potentials even for single-component SAMs. The origin of the subwave is presently unclear but is probably due to the heterogeneity in the crystallinity of the substrate surface[64] and in the packing of thiol molecules[64,66] as disscussed in the previous paper.[30] As expected for shorter chain and hydrophilic SAM, the MPA SAM was desorbed at the most positive potential. Alkanethiol SAMs were desorbed at more negative

(63) (a) Poirier, G. E.; Tarlov, M. J.; Rushmeier, H. E. *Langmuir* **1994**, *10*, 3383. (b) Poirier, G. E.; Tarlov, M. J. *J. Phys. Chem.* **1995**, *99*, 10966. (c) Poirier, G. E.; Pylant, E. D. *Science* **1996**, *272*, 1145. (d) Poirier, G. E. *Langmuir* **1997**, *13*, 2019.
(64) (a) Widrig, C. A.; Chung, C.; Porter, M. D. *J. Electroanal. Chem.* **1991**, *310*, 335. (b) Walczak, M. M.; Popenoe, D. D.; Deinhammer, R. S.; Lamp, B. D.; Chung, C.; Porter, M. D. *Langmuir* **1991**, *7*, 2687. (c) Weisshaar, D. E.; Lamp, B. D.; Porter, M. D. *J. Am. Chem. Soc.* **1992**, *114*, 5860. (d) Zhong, C.-J.; Zak, J.; Porter, M. D. *J. Electroanal. Chem.* **1995**, *396*, 103. (e) Walczak, M. M.; Alves, C. A.; Lamp, B. D.; Porter, M. D. *J. Electroanal. Chem.* **1997**, *421*, 9. (f) Zhong, C.-J.; Porter, M. D. *J. Am. Chem. Soc.* **1994**, *116*, 11616. (g) Zhong, C.-J.; Zak, J.; Porter, M. D. *J. Electroanal. Chem.* **1997**, *421*,9. (h) Zhong, C.-J.; Porter, M. D. *J. Electroanal. Chem.* **1997**, *425*, 147.
(65) Calvente, J. J.; Kovacova, Z.; Sanchez, M. D.; Andreu, R.; Fawcett, W. R. *Langmuir* **1996**, *12*, 5696.
(66) (a) Yang, D.-F.; Wilde, C. P.; Morin, M. *Langmuir* **1997**, *13*, 243, (b) Yang, D.-F.; Wilde, C. P.; Morin, M. *Langmuir* **1996**, *12*, 6577.
(67) Pan, J.; Tao, N.; Lindsay, S. M. *Langmuir* **1993**, *9*, 1555.
(68) Schneider, T. W.; Buttry, D. A. *J. Am. Chem. Soc.* **1993**, *115*, 12391.
(69) Becka, A. M.; Miller, C. J. *J. Phys. Chem.* **1993**, *97*, 6233.

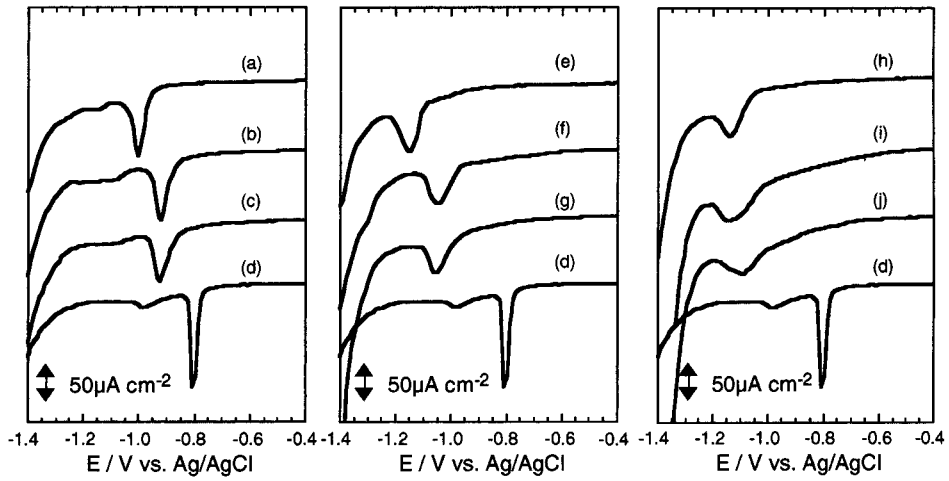

Figure 7. Reductive desorption of single-component monolayers and mixed mercaptopropionic acid/alkanethiol monolayers in 0.5 M KOH with a sweep rate of 0.10 V s^{-1}. (a) Octanethiol SAM, (b, c) mixed mercaptopropionic acid/octanethiol monolayers, (d) mercaptopropionic acid SAM, (e) dodecanethiol SAM, (f, g) mixed mercaptopropionic acid/dodecanethiol monolayers, (h) octadecanethiol SAM, and (i, j) mixed mercaptopropionic acid/octadecanethiol monolayers. Initial surface Pb coverages: (b, f, i) 0.30; (c, g, j) 0.60.

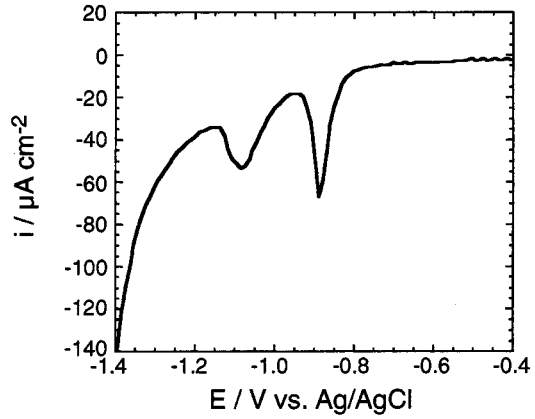

Figure 8. Reductive desorption of mixed mercaptopropionic acid/dodecanethiol monolayers prepared from 1 mM mixed solution of mercaptopropionic acid and dodecanethiol (solvent, ethanol; immersion time, 1 h). Electrolyte solution, 0.5 M KOH; sweep rate, 0.10 V s^{-1}.

potentials, and the desorption potential is dependent on the chain length; a longer alkanethiol is desorbed at a more negative potential.[64] Mixed monolayers also give voltammograms similar in shape to those of single-component SAMs. Either peak splitting or two waves, which are common features for mixed monolayers consisting of single-component domains,[13−15] were not observed. Therefore, no evidence exists showing that the domain formation takes place. For comparison, the voltammogram for the reductive desorption of the mixed MPA/dodecanethiol monolayer prepared by immersing the electrode in a mixed solution is shown in Figure 8. Two peaks, assigned to the desorption of the corresponding single-component SAMs, appeared as expected for the formation of the domains. Therefore, the difference between mixed monolayers prepared by the present and the traditional method is distinct. The desorption charge for mixed monolayers prepared by the present method was determined in the manner described above. PZCs and capacitances used in the calculations are listed in Table 1. Compared with Q_{des} before the adsorption of MPA, the charge increased to the value expected for a monolayer and is almost independent of the chain length of the alkanethiol. These values after taking the roughness factor into account (113−94 μC cm^{-2}) are close to that expected for the $(\sqrt{3}\times\sqrt{3})R30°$ structure. A linear relation exists between Q_{des} and the initial Pb coverage (Figure 9a). These results show that MPA is adsorbed on vacant sites on Au, which is created by desorption of the UPD Pb.

XPS O 1s spectra of the mixed and single-component monolayers were taken just after the construction. The O 1s intensity increased with the initial Pb coverage or the fraction of vacant sites. The integrated intensity is plotted versus θ_{Pb}^{0} (Figure 9b). A linear relationship exists between them, showing that the surface fractions of MPA are the same as the initial Pb coverage. Therefore, it is also confirmed from XPS measurements that the surface coverage of MPA in the mixed monolayers is determined by the initial Pb coverage.

The FT-IR spectrum of the mixed octadecanethiol/MPA monolayer is shown in Figure 4d. The band intensity is weaker than that of the octadecanethiol adlayer with vacant sites (Figure 4c). However, the intensity becomes close to the value expected from the surface composition and the intensity of the SAMs on Au and UPD Pb/Au (Figure 4a and b). For $\nu_a(CH_2)$, as an example, the intensity is expected to be 46% of that for the SAMs (for the sample shown in Figure 4d, the surface composition is 60% octadecanethiol and 40% MPA, and therefore, the number of CH_2 units becomes $(60 \times 17 + 40 \times 2)/17 = 46\%$ of that for the single-component octadecanethiol SAMs). The observed intensity is 41% of that for the SAMs. Taking into account that an MPA SAM does not give a clear peak (Figures 4e), the intensity becomes closer to the expected one (40%). Because the surface composition of this sample (60% MPA) is confirmed by XPS and the reductive desorption, the change in the band intensity by the adsorption of MPA (compare Figure 4c and d) is due to the change in the orientation of the alkyl chain from a less perpendicular to a more perpendicular one (back to the original orientation). This change is induced by MPAs occupying the vacant rows next to the alkanethiol rows. The $\nu_a(CH_2)$ band shifted to 2920 cm^{-1} for the mixed monolayer from 2918 cm^{-1} for the SAMs on Au and UPD Pb/Au, and octadecanethiol adlayer with vacant sites. Because this band is the most sensitive among the CH stretching modes to the crystallinity of the thiol layer (2924 cm^{-1} for liquid and 2918 cm^{-1} for crystalline state),[61] the observed shift indicates

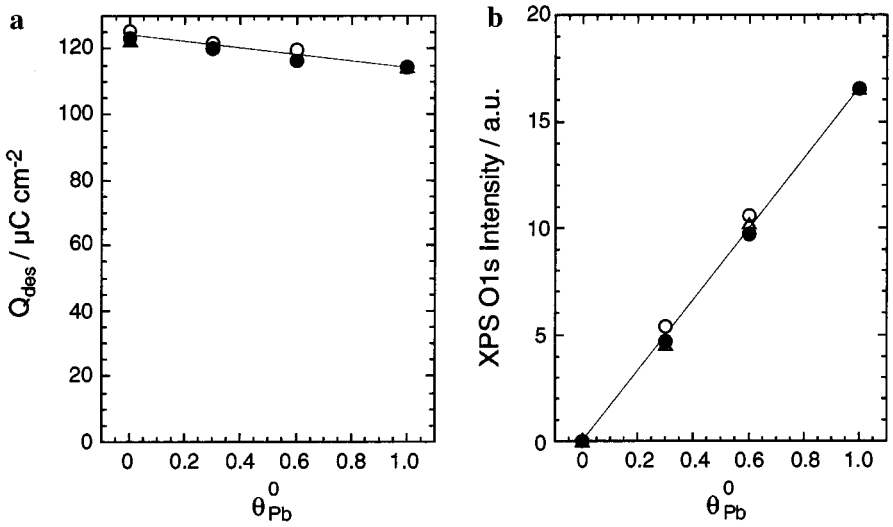

Figure 9. (a) Desorption charge and (b) XPS O 1s intensity of mixed mercaptopropionic acid/alkanethiol monolayers as a function of initial Pb coverage. Alkanethiols: octanethiol (open circle), dodecanethiol (solid circle), and octadecanethiol (triangle).

that the adsorbed layer becomes somewhat disordered upon the adsorption of MPA. In addition to the bands in the C—H region, the new band appeared at around 1700 cm^{-1} (not shown), which is due to the C═O stretching of COOH.[58,70−73] The intensity of this band is 64% of that for a single-component MPA SAM, which agrees with the initial Pb coverage of this sample ($\theta_{Pb}^0 = 0.60$). Therefore, this also supports the adsorption of MPA.

Figure 10a shows a typical 23.6 × 23.6 nm^2 STM image of mixed MPA/octanethiol monolayers. Pinstriped domains were observed in the image. The domain size is approximately 4−10 nm along the axis of the pinstripe and 5−15 nm wide. The rows in the adjacent pinstriped domains intersect at an angle of 60 or 120°, which agrees with the symmetry of the underlying Au(111) lattice. A disordered region also exists, the surface fraction of which varies from sample to sample, but is typically less than 30%. This fraction is clearly larger than those observed for the SAMs on UPD Pb/Au and the adlayer with 60% vacant sites (not shown). The adsorption of MPA probably induces the adlayer to be more disordered. This result is consistent with the positive shift in the $\nu_a(CH_2)$ band observed in the FT-IR spectra. The pits observed as dark holes are due to the vacancy islands of the surface as reported in the literature,[63a,74] because the depth of the pits is close to that of the monatomic step of the Au(111) surface. We have never observed the domains that can be assigned to single-component domains of MPA and octanethiol (It is reported that the single-component monolayer of MPA exhibits rhombic (3 × 3).[75]

A high-resolution image of the pinstriped domains is shown in Figure 10b. Compared with the STM image before the adsorption of MPA, it is clear that dimmer spots appear in the space between the rows of bright spots, indicating the adsorption of MPA. The periodicity along the row was maintained at ∼0.49 nm. The spacing between two adjacent bright rows is 0.85−1.01 nm, showing that some of the spacing expands with the adsorption of MPA.

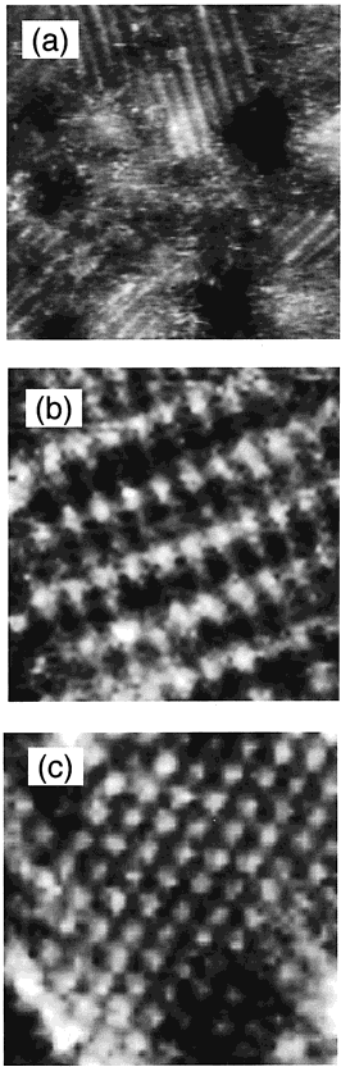

Figure 10. (a, b) STM images of mixed monolayers of MPA and octanethiol: (a) 23.6 nm × 23.6 nm; (b) 5 nm × 5 nm. (c) A STM image of mixed octanethiol/octanethiol monolayer (see text for detail). The initial Pb coverage is 0.60.

(70) Cheng, S. S.; Scherson, D. A.; Sukenik, C. N. *Langmuir* **1995**, *11*, 1190.
(71) Troughton, E. B.; Bain, C. D.; Whitesides, G. M.; Nuzzo, R. G.; Allara, D. L.; Porter, M. D. *Langmuir* **1988**, *4*, 365.
(72) Smith, E. L.; Porter, M. D. *J. Phys. Chem.* **1993**, *97*, 8032.
(73) Tao, Y.-T.; Hietpas, G. D.; Allara, D. L. *J. Am. Chem. Soc.* **1996**, *118*, 6724.
(74) Yamada, R.; Uosaki, K. *Langmuir* **1998**, *14*, 855.
(75) Sawaguchi, T.; Sato, Y.; Mizutani, F. *J. Electroanal. Chem.* **2001**, *496*, 50.

One might think that the pinstripe originates from the single-component SAM, because the spots between the bright rows is not well-resolved and because a considerable number of studies reported the existence of the pinstriped structure in single-component SAMs of alkanethiol and their derivatives.[63,74,76−83] For the pinstripes observed at the initial stage of SAM formation or after annealing the SAM of the $(\sqrt{3}\times\sqrt{3})R30°$ structure at elevated temperatures, it was proposed that the thiol molecules lie on the surface or align along the substrate surface.[63c,82,83] The pinstripe was also observed for the unannealed SAM with high coverage of the thiol. In this case, the pinstripe can be created by translating the row from the $(\sqrt{3}\times\sqrt{3})R30°$ sites to the next-nearest-neighbor sites, resulting in a wider gap between the rows.[63a,80] For several reasons, it is clear that MPA molecules exist in the region between the rows. Namely, the spacing is not a real missing row. First, there are dimmer spots in the region as described above. Second, we have never observed the pinstripe structure in STM images of single-component SAMs prepared under conditions of thiol concentration and immersion time similar to those for mixed monolayers. Third, the adsorption of MPA was confirmed by reductive desorption voltammetry and XPS. To confirm the adsorption of the second thiol by STM, in addition, we have prepared a mixed octanethiol/octanethiol monolayer using octanethiol as the second thiol species instead of MPA. The result is shown in Figure 10c. If octanethiol molecules are not adsorbed on the vacant sites, a pinstripe would appear in the STM images. However, a pinstripe was not observed, and instead, the domains of the $(\sqrt{3}\times\sqrt{3})R30°$ structure appeared, showing the adsorption of the second thiol species.

In summary, the surface coverage of MPA in the mixed monolayers with alkanethiols is the same as that of the lead underpotentially deposited at the first step of the construction procedure proposed here, as confirmed by XPS and reductive desorption voltammetry. A single desorption peak observed in reductive desorption voltammograms demonstrates that MPA and alkanethiol are mixed homogeneously. The STM images reveal the existence of the pinstripe structure, showing the mixing of the component thiols at the molecular level. We have also constructed the mixed monolayers of alkanethiols and other functionalized thiols such as aminoethanethiol, ferrocenyl-undecanethiol, and thiol-derivatized metalloporphyrin.[84] XPS and reductive desorption voltammetry demonstrated that the surface coverages of these functionalized thiols can be determined by the initial Pb coverage as in the case of MPA/alkanethiol mixed monolayers. Therefore, the present method is generally useful for creating mixed monolayers with controlled composition. To develop the novel concept proposed here, we are now attempting to use the other UPD metals and organic molecules as controlling elements.

Acknowledgment. We thank Prof. K. Uosaki and Dr. R. Yamada of Hokkaido University for their instruction on the STM measurements. This work is partially supported by a Grant-in-Aid for Scientific Research and for Priority Area Research of "Electrochemistry of Ordered Interfaces" from the Ministry of Education, Science, Sports and Culture, Japan.

JA004091B

(76) Schonenberger, C.; Sondag-Huethorst, J. A.; Jorritsma, J.; Fokkink, L. G. *Langmuir* **1994**, *10*, 611.
(77) Delamarche, E.; Michel, B.; Kang, H.; Gerber, Ch. *Langmuir* **1994**, *10*, 4103.
(78) Dishner, M. H.; Hemminger, J. C.; Feher, F. J. *Langmuir* **1996**, *12*, 6176.
(79) Nakamura, T.; Kondoh, H.; Matsumoto, M.; Nozoye, H. *Langmuir* **1996**, *12*, 5997.
(80) Kang, J.; Rowntree, P. A. *Langmuir* **1996**, *12*, 2813.
(81) Yamada, R.; Uosaki, K. *Langmuir* **1997**, *13*, 5218.
(82) Touzov, I.; Gorman, C. B. *Langmuir* **1997**, *13*, 4850.
(83) Staub, R.; Toevker, M.; Fritz, T.; Schmitz-Hubsch, T.; Sellan, F.; Leo, K. *Langmuir* **1998**, *14*, 6693.
(84) Kawaguchi, T.; Shimazu, K.. in preparation.